# Conversions over Low Barriers. 8. The Mechanism and Rate of Dissociation of Dimeric Formic Acid

**D. Borchardt, J. F. Caballero, and S. H. Bauer***

*Contribution from the Department of Chemistry, Baker Laboratory, Cornell University, Ithaca, New York 14853-1301.* *Received March 11, 1987*

**Abstract:** Dissociation rates of dimeric formic acid in the gas phase were measured over the temperature range 293–335 K, via T-jump experiments. Since the He/Ne laser line at 3.3913 μm is selectively absorbed by the dimer, changes in its intensity permit measurement on a μs time scale of relaxation times of dimer/monomer mixtures to their new equilibrium ratios, when perturbed by injection of small amounts of energy by a $CO_2$ laser. Initial formic acid pressures ranged from 1.0 to 2.75 Torr. Relaxation to equilibrium followed single exponential decays, which did not depend on whether the monomer or dimer was irradiated. The thermochemical parameters for dissociation are well documented: $\Delta H°_{300}$ = 15.25 kcal/mol and $\Delta S°_{300}$ = 39.24 eu. However, the measured activation energy is 7.4 ± 1 kcal/mol. Furthermore, even though at the pressures used the system should be in the second order regime, the addition of 10–600 Torr of Ar had no measurable effect on the rate. These observations can be reconciled by assuming that (i) the ring structure opens when a (free) monomer adds to one of the O···HO bonds in the dimer, thereby releasing one of the initial monomers and generating a chain dimer, and that (ii) the latter relatively rapidly dissociates into two monomers. That dissociation was catalyzed by short-lived [O···HO] adducts was demonstrated by measuring relaxation times in the presence of added species: $(CD_3)_2CO$, THF-$d_8$, $(CH_2)_3O$, and $(CH_2)_2O$. $\tau$'s declined linearly with the pressure of the diluent.

During the 75 years since the concept of H bonds was introduced,[1] a myriad of conjectures, calculations, and experiments have dealt with the essential features of this type of bonding, their geometric structures,[2] the energetics, and spectroscopy.[3] However, very few experiments have been devoted to the dynamics of the association/dissociation process, in contrast to the numerous theoretical analyses that were published concerning the dynamics of hydrogen atoms in two-well potentials generated by bond formation.[4] For acetic acid solutions ultrasonic relaxation measurements indicated that the cyclic dimer dissociates stepwise, first to an open chain and subsequently to the monomers.[5] The dimer/monomer dissociation of gaseous formic acid was investigated by shock heating.[6] Since the temperature increment ranged from 20 to 80 °C, equilibrium was attained within the shock front, and only an upper limit for the relaxation time was obtained (1–2 μs). On this basis sequential bond breaking of the cyclic structure was proposed. This was later supported by a T-jump experiment with acetic acid;[7] the reported activation energy is 11.4 ± 0.9 kcal/mol.

The following is a partial list of basic questions which remain: (i) Are the activation energies for dissociation greater than, equal to, or less than the established bond energies? (ii) In particular, for the aliphatic acids (ring structures) if the bonds open sequentially, what are the lifetimes of the singly bonded species? (iii) Does RRKM theory accurately account for the dissociation? (iv) At what low pressure does the kinetics of the dissociation switch from first to second order? (v) Is it possible to photodissociate these weak bonds by direct absorption of IR radiation at the bond site? (vi) Since at ambient temperatures and pressures equilibrium is maintained between the component species and their associated complex, what other low-barrier processes that are generally present (such as rotations of single bonds) couple to the dissociation dynamics? Some, but not all, of these questions would be answered were temperature-dependent relaxation times measured for the dissociation/association process.

This report concerns measurements of dissociation–association relaxation rates in gaseous formic acid at low pressures (1.0–2.75 Torr, with variously added levels of argon, $SF_6$, and other diluents) following *small* temperature jumps induced by microsecond $CO_2$ laser pulses. Our previous attempt to deduce the kinetics of this system from NMR relaxation times[8] failed, in that we could only establish an upper bound for the activation energy for the overall dissociation step. This proved to be somewhat less than 12 kcal/mol, in contrast to the established $\Delta H°_{300}$ = 15.25 ± 0.3 kcal/mol.[9] RRKM calculations (assuming $E_0 \approx$ 12–9.5 kcal/mol) show that at pressures below ≈10 Torr the system should be in the second-order regime.

## Experimental Protocol

From our NMR studies we anticipated that the system relaxation times at room temperature would be in the range of ≈10 μs. Hence perturbation pulse durations and diagnostic response times were set at somewhat less than 1.0 μs. Well-resolved FTIR spectra (0.25 $cm^{-1}$) facilitated the selection of characteristic frequencies. Figure 1 shows the absorption spectra of an equilibrium mixture (1) and of the resolved spectra of the dimer (2) and monomers (3).[10] The He/Ne laser line at 3.3913 μm coincides with the intense C–H stretching absorption band of the dimer (presumed to be the symmetric ring structure) and with the *band center* (minimum absorption) of the C–H band of the monomer. Hence changes in transmissions of He/Ne radiation, recorded with a fast InSb detector (≈0.5 μs) [→ Biomation transient digitizer → TraCor Northern multichannel analyzer → computer], measure directly the amount of dimer present in the experimental cell as a function of time.

(1) Hantzsch, A. *Ber.* **1910**, *43*, 3049; **1911**, *44*, 1771.
(2) A recent theoretical analysis was presented by Karpfen: Karpfen, A. *Chem. Phys.* **1984**, *88*, 415.
(3) Sandorfy, C. *Top. Current Chem.* **1984**, *120*, 41. Also: *Molecular Interactions*, Ratajczak, Orville-Thomas, W. J., Redshaw, M., Eds.; John Wiley and Sons: Chichester, 1981; Vol. 2.
(4) A few of the latest contributions to the extensive literature follow: (a) Carmeli, B.; Nitzan, A. J. *J. Chem. Phys.* **1984**, *80*, 3596. (b) Siebrand, W.; Wildman, R. A.; Zgierski, M. Z. *J. Am. Chem. Soc.* **1984**, *106*, 4083, 4089. (c) Baughcum, S. L.; Smith, Z.; Wilson, E. B.; Duerst, R. W. *J. Am. Chem. Soc.* **1984**, *106*, 2260. (d) Rothschild, W. G. *J. Chem. Phys.* **1974**, *61*, 3422. (e) Meier, B. H.; Graf, F.; Ernst, R. R. *J. Chem. Phys.* **1982**, *76*, 767; **1981**, *75*, 2914. (f) Meier, B. H. et al. *Chem. Phys. Lett.* **1983**, *103*, 169. (g) Nagaoka, S. et al. *Phys. Lett.* **1981**, *80*, 580; *J. Chem. Phys.* **1983**, *79*, 4694. (h) Lipinski, J.; Sokalski, W. A. *Chem. Phys. Lett.* **1980**, *76*, 88. (i) Exchange of comments between Furic, Meir, and Nagaoka: Furic, K.; Meir, B. H.; Nagaoka, A. *Chem. Phys. Lett.* **1984**, *108*, 518–525. (j) Hayaski, S.; Umemura, J.; Kato, S.; Morokuma, K. *J. Phys. Chem.* **1984**, *88*, 1330–1334. Meyer, R.; Ernst, R. R. *J. Chem. Phys.* **1987**, *86*, 784.
(5) Carsaro, R. D.; Atkinson, G. *J. Chem. Phys.* **1971**, *54*, 4090.
(6) Galubev, N. S.; Denisov, G. S.; Shimkus, R. *Khim. Fiz.* **1982**, *7*, 967.
(7) Voronin, A. U.; Gerasimov, I. V.; Denisov, G. S.; Rutkovski, K. S.; Tokhadze, K. G. *Chem. Phys. Lett.* **1983**, *101*, 197. A temperature-jump measurement of the relaxation time of the $N_2O_4 \rightleftharpoons 2NO_2$ system was reported by Gozel et al.: Gozel, P.; Calpini, B.; van denBergh, H. *Isr. J. Chem.* **1984**, *24*, 210.
(8) Lazaar, K. I.; Bauer, S. H. *J. Am. Chem. Soc.* **1985**, *107*, 3769.
(9) Waring, W. *Chem. Rev.* **1952**, *51*, 171. Chao, J.; Zwolinski, B. J. *J. Phys. Chem. Ref. Data* **1978**, *7*, 363.
(10) Wachs, T.; Borchardt, D.; Bauer, S. H. *Spectrochim. Acta* **1987**, *43A*, 965.

0002-7863/87/1509-6651$01.50/0 

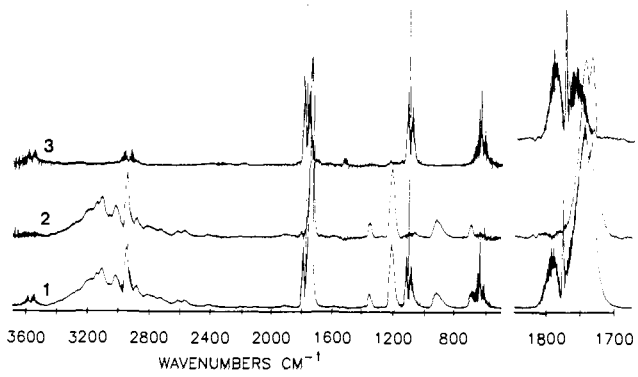


**Figure 1.** FTIR spectra of gaseous formic acid: (1) 4.9 Torr of monomer–dimer equilibrium mixture (10 cm cell), (2) resolved *dimer* spectrum, and (3) resolved *monomer* spectrum.

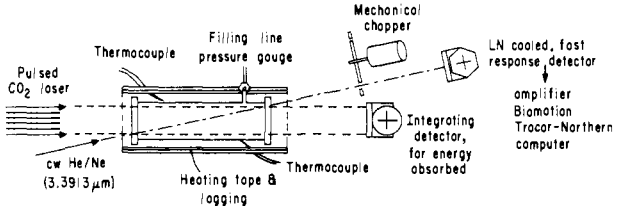


**Figure 2.** Schematic of experimental arrangement.

This was confirmed by direct calibration.

Figure 2 is a schematic of the experimental arrangement. The cell [either 2 or 3 cm i.d. and 10 or 15 cm long, respectively] was wrapped with a heating tape and lagged; several thermocouples were installed adjacent to the glass surface. Formic acid vapor was admitted to the cell; after sufficient time was allowed for establishing equilibrium, allowing for adsorption onto the inner surfaces of the cell, pressures were read with an MKS Baratron [170M-6A] capacitance manometer. No significant changes were found when the cell was pretreated with $(CH_3)_3SiCl$. For calibration, the mechanical chopper was turned on, and the ac signal was read at the TraCor Norther after an accumulation of 64 pulses, with the cell empty and when filled to a known pressure [range 1.0–2.75 Torr + up to 600 Torr diluent] and temperature [range 293.5–330 K]. Absorptions by the cell contents were thus determined. Absorbances were independent of the total pressure and temperature but were linearly dependent on the calculated *dimer* concentration derived from $K_{eq}(T)$ values,[9] based on $\Delta H°_{dis}$ = 15.25 kcal/mol and $\Delta S°_{dis}$ = 39.24 eu, as shown in Figure 3. This plot enables us to reverse the process, to deduce the equilibrated gas-phase temperature for any known formic acid gas density and recorded absorbance. The He/Ne laser output was somewhat less than 2 mW; less than 30% is absorbed by 2.0 Torr of formic acid. Since the kinetic measurements were made under steady illumination by the He/Ne laser, this relatively small energy input merely raises slightly the initial temperature in the vicinity of the narrow He/Ne beam.

Carbon dioxide laser lines are also absorbed by formic acid. Its infrared spectrum is shown on an expanded scale in Figure 4 [1400 → 800 $cm^{-1}$]. Attention is called to the possibility of selectively irradiating the dimer band at 975 $cm^{-1}$ or the monomer band in the 1100-$cm^{-1}$ region; care must be taken to avoid the weak $\nu_{13}[\gamma(C-H)]$ of the dimer situated at ≈1045 $cm^{-1}$ under the P-branch of the monomer. A few runs were made with R28-R32 of the 10.6-μm band near the minimum absorbance region [982.13 $cm^{-1}$]. For these we added $SF_6$ to serve as a heat-transfer agent; its weak band at 983.25 $cm^{-1}$ is also shown in Figure 4. The line tunable $CO_2$ laser is a Lumonics TEA, K-103, which was operated at an output of ≈750 mJ per pulse, with pulse durations (fwhm ≈ 0.5 μs, with a low intensity tail). Pressures in the cell were kept low (1.0 → 2.75 Torr) to ensure uniform heating thruout its entire length. Also, we found that when the pressure of formic acid exceeded about 3 Torr, density oscillations were set up, presumably due to the steeply rising front of the irradiating pulse.[11]

Each run was started by recording the intensity of the He/Ne laser through the empty cell (chopper on, $I_0$) and similarly through the filled cell ($I_i$). The He/Ne laser intensity was checked at the beginning and at the end of each run. This proved essential because of drift in laser output. Then, under constant illumination by the He/Ne laser, line selected $CO_2$ laser pulses were incident on the filled cell, triggering the Biomation unit (generally 64 shots were accumulated). The digitized He/Ne signal was recorded as a function of time. Figure 5a is an expanded plot of the rising part of the signal; the increased transmission is a measure of the time-dependent depletion of the dimer. These curves are well fitted by a single exponential function

$$I(t) = (I_i - I_\infty) \exp(-|t - t_0|/\tau) + I_\infty \quad (1)$$

From the magnitude of $(I_\infty - I_i)$ and the known initial pressure and temperature one can calculate the temperature rise imposed by the absorbed $CO_2$ laser radiation. [Use of intensities, rather than absorbances, is valid in this case, since Δ(dimer)/dimer is small.] Table I is a summary of the experimental parameters for the various runs and the deduced relaxation times, $\tau$.

Figure 5b is a typical decay curve; it shows that the cell composition returns to its initial state in about 0.1 s, due to heat conduction to the cell walls. This is consistent with cooling rates we previously found for laser heated methyl formate.[12] Finally we note that tests were made to establish that the changes in intensities we recorded were not due to thermal lensing.

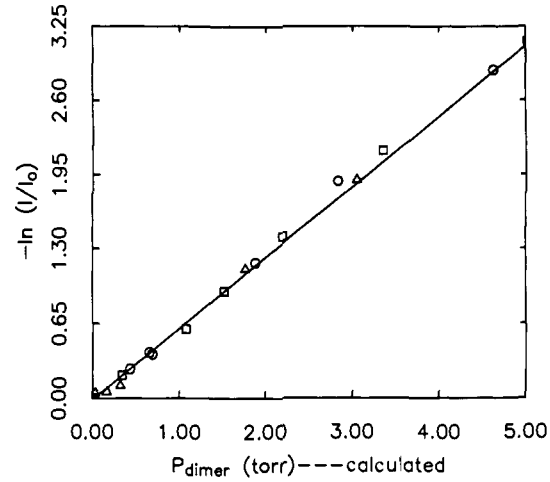


**Figure 3.** Beer's law plot for formic acid dimer, at 3.3913 μm: (Δ) 320.0 K, (○) 305.5 K, (□) 296.5 K. The slope = 0.617; intercept = $-8.0 \times 10^{-3}$; $l$ = 16 cm, $\epsilon$ = 0.0386 $cm^{-1}$ $Torr^{-1}$.

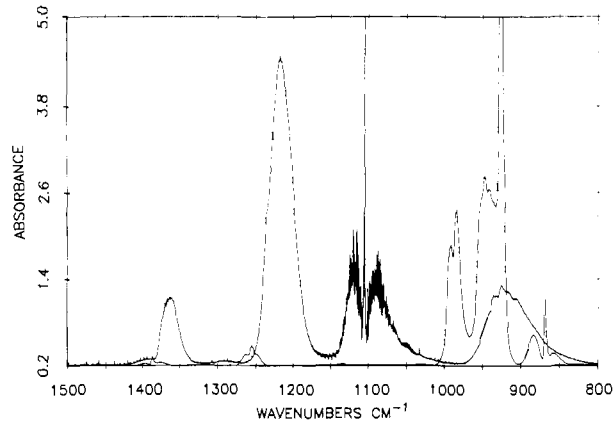


**Figure 4.** FTIR spectrum of the 1150–800-$cm^{-1}$ region of the formic acid (equilibrium mixture). The peaks at 985 and 940 $cm^{-1}$ are of $SF_6$.

## Discussion

The sequence of molecular structures assumed during the dissociation event is most readily described in terms of the inverse of the sequence followed during the association of two monomers. As is well-known, formic acid monomers (Γ) exist in two conformations, with the trans configuration more stable than cis by about 3.9 kcal/mol.[13] Hence the ratio cis/trans ≈ $1.5 \times 10^{-3}$

(11) Diebold, G. J. *J. Phys. Chem.* **1980**, *84*, 2213. Gucker, J. R.; Carr, P. W. *J. Phys. Chem.* **1986**, *90*, 4286. Karbach, A.; Hess, P. *J. Chem. Phys.* **1986**, *84*, 2945.

(12) Ruschin, S.; Bauer, S. H. *J. Phys. Chem.* **1980**, *84*, 3061.

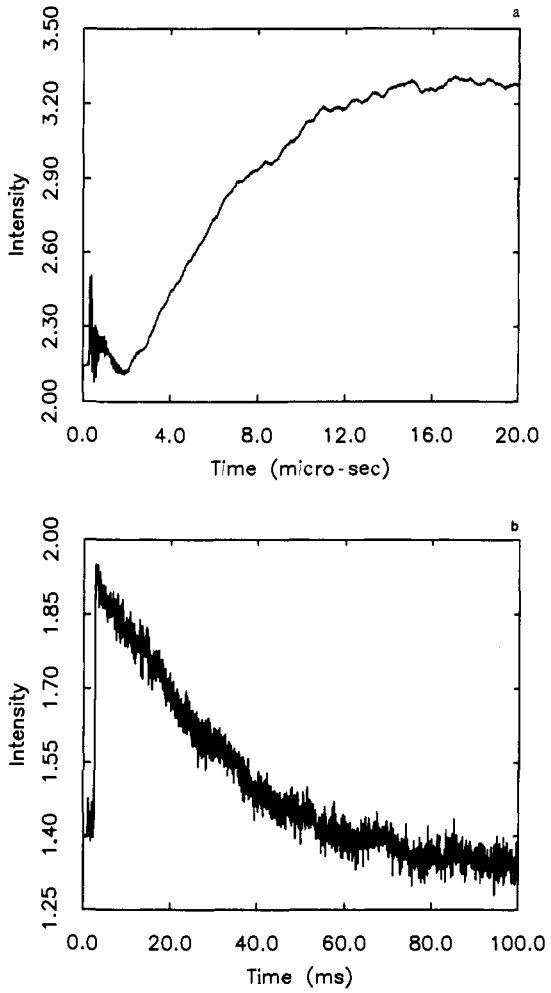


**Figure 5.** Typical time profile of the He/Ne intensity. The initial fast rise is due to relaxation of the system to the new equilibrium state as dictated by the rapid temperature jump. (a) Time profile of the transmitted He/Ne intensity on a μs time scale. (b) The much slower decay is due to cooling of the cell contents back to the initial cell temperature.

at room temperature. The association of (c + c) or (c + t) generates a chain (designated Ω), whereas only a properly oriented pair (t + t) can produce the conventional ring structure ($\phi$). Of course, the nascent Ω or $\phi$ species must be collisionally stabilized. In reverse, when an $\phi$ species accumulates sufficient energy in the ring vibrations one of the OH---O bonds may open, but if unperturbed it will eventually close again because the rotational barrier about the HO–C bond is ≈13.8 kcal/mol.[14] At 300 K we estimate $\Delta H^\circ_{300}(\phi \rightarrow \Omega) \approx 8.5$ kcal/mol; $\Delta S^\circ_{300}(\phi \rightarrow \Omega) \approx 22$ eu. Hence, at equilibrium, the ratio $\{[\Omega]/[\phi]\}_{eq} = K^{(300)}_{\phi\rightarrow\Omega} = 0.041$. This low level is not inconsistent with our being unable to detect the Ω configuration in the NMR spectrum,[8] but it may be detectable via its microwave spectrum. For the ring/monomer equilibrium

$$K^{(p)}_{\phi\rightarrow\Gamma} = e^{+39.24/R}e^{-15250/RT};\ K^{(c)}_{\phi\rightarrow\Gamma} = K^{(p)}_{\phi\rightarrow\Gamma}/RT \qquad (2)$$

Let $n$ be the total mol/cm³; then

$$[\phi] = n\{(1-\alpha)/(1+\alpha)\};\ [\Gamma] = n\{2\alpha/(1+\alpha)\} \qquad (3a)$$

$$\alpha = [K^{(c)}/(4n + K^{(c)})]^{1/2} \qquad (3b)$$

The estimated $\Omega/\phi$ ratio should be compared to the concentration ratio of monomer-to-ring dimer; $[\Gamma]/[\phi] = 1.12$ at 300 K; it rises to 1.61 at 310 K for $n = 1.07 \times 10^{-7}$ mol/cm³. Figure 6a,b illustrates the distribution of populations for the $\phi$ species, as a

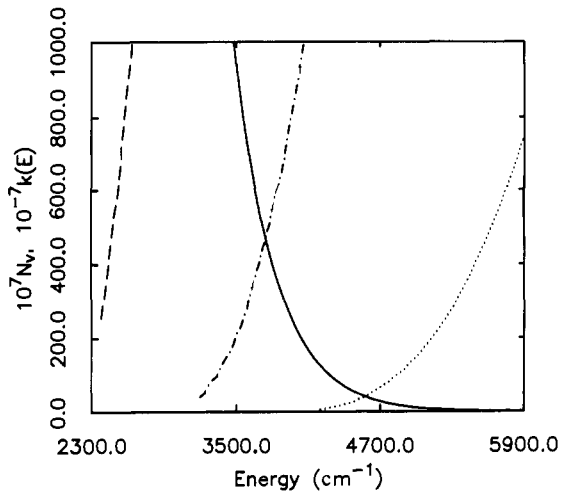


**Figure 6.** Population distribution as a function of total vibrational energy at 300 K for the ring dimer. Also shown are plots of $k(E)$ for various values of $E^\circ$. The $N_v$ values are populations integrated over 50-cm⁻¹ intervals. The plotted values are $10^7$ times those calculated; similarly (for scaling), the $k(E)$ values were multiplied by $10^{-7}$. To obtain fractional populations over extended ranges of energy, $P = \int_{\nu_1}^{\nu_2} N_v\, d\nu$ was evaluated for the following: (—) $N_v$; $(\nu_2 - \nu_1) = 2380 \rightarrow 3200$ cm⁻¹, $P = 1.55 \times 10^{-2}$, (– – –) $k(E)$, $E^\circ = 2380$ cm⁻¹; $(\nu_2 - \nu_1) = 3200 \rightarrow 4200$ cm⁻¹, $P = 2.01 \times 10^{-3}$, (–·–·) $k(E)$, $E^\circ = 3200$ cm⁻¹; $(\nu_2 - \nu_1) = 4200 \rightarrow \infty$ cm⁻¹, $P = 1.17 \times 10^{-3}$, (···) $k(E)$, $E^\circ = 4200$ cm⁻¹.

function of total vibrational energy, at 300 K. Integrated values at several levels of excitation are indicated. The vibrational frequencies for $\phi$ were taken from the assignments by Kirklin et al.[15]

Prelude to an analysis of the observed relaxation times, consider both inter and intra energy transfer rates, which control the conversion of vibrational excitation induced by the absorbed $CO_2$ laser photons to the reaction coordinate that is involved in dissociation. In the absence of directly measured $v \rightarrow RT$ relaxation times for formic acid one can estimate from Lambert–Salter plots[16] and use tabulated values for analogous species ($H_2O$; $CH_3OH$). We propose the following reasonable values for $Z_{10}$ at 300 K (mean number of collisions required to de-energize a molecule from the first excited vibrational state to the ground level).

$$\begin{aligned} \phi^{(1)} + \Gamma &\rightarrow \phi + \Gamma + (\text{ke; rot}) \quad Z_{10} = 5 \\ \phi^{(1)} + \phi &\rightarrow \phi + \phi + (\text{ke; rot}) \quad Z_{10} = 10 \\ \phi^{(1)} + \text{Ar} &\rightarrow \phi + \text{Ar} + (\text{ke; rot}) \quad Z_{10} = 10^2 \\ \Gamma^{(1)} + \Gamma &\rightarrow \Gamma + \Gamma + (\text{ke; rot}) \quad Z_{10} = 5 \end{aligned} \qquad (4)$$

ke = kinetic energy

Thus for $p \approx 1$ Torr of formic acid plus ≈10 Torr of argon, $\tau_{v\rightarrow RT} \approx 10^{-6}$ s. It is unreasonable to postulate that the IVR rate is slower than the $v \rightarrow RT$ rate, since there are indications that H-bonding interactions enhance the relaxation efficiency ($\tau_v^{-1}$) of H–X valence modes.[17]

We considered the consequences of the fact that the absorbance measured is due solely to the population of the $\nu_{18}$(C–H) oscillators in their *ground state*, even subsequent to a pulse of injected energy by the $CO_2$ laser. Rapid $v \rightarrow RT$ relaxation occurs so that the overall temperature is raised. Were there no dissociation of the dimer, absorption of the 3.39-μm He/Ne line would decrease

(13) Hocking, W. H. *Z. Naturforsch.* **1976**, *31a*, 1113.
(14) Winnewisser, B. P.; Hocking, W. H. *Z. J. Phys. Chem.* **1980**, *84*, 1771.
(15) Kirklin, D. R.; Lippincott, E. R.; Khanna, R. H., based on the Ph.D. dissertation of D. R. Kirklin, University of Maryland, College Park, 1975, "Spectroscopic Investigations of Hydrogen Bonded Vapors". Refered to by: Bosi, P.; Zerbi, G. *J. Chem. Phys.* **1977**, *66*, 3376. Recently high-resolution spectra of formic acid have been reported: Man, H.-T.; Butcher, R. J. *J. Mol. Spectrosc.* **1984**, *107*, 284. Weber, W. H.; Maker, P. D.; Johns, J. W. C.; Weinberger, E. *J. Mol. Spectrosc.* **1987**, *121*, 243.
(16) Lambert, J. D. *Vibrational and Rotational Relaxation in Gases*; Claredon: Oxford, 1977.
(17) Hadzi, H.; Bates, S. In *The H-Bond, II*; Schuster, P., Zindel, G., Sandorfy, C., Eds.; North-Holland: Amsterdam, 1976; p 565.

**Table I.** Experimental Conditions and Relaxation Times for the Formic Acid Dissociation

| run no. | $\lambda_{CO_2}$ ($cm^{-1}$)[a] | $T_0/T_f$ (K) | $P_0$ (Torr) monomer/dimer | diluent[b] $P$ (Torr) | $P_f$ (Torr) monomer/dimer | $10^6\tau$ (s) |
|---|---|---|---|---|---|---|
| 1 | 1085.75 | 295.0/298.2 | 0.80/0.45 | 7.05 | 0.88/0.41 | 6.85 |
| 2 | 1085.75 | 294.8/298.4 | 0.77/0.43 | 4.49 | 0.86/0.38 | 6.30 |
| 3 | 1085.75 | 297.0/300.8 | 1.47/1.28 | 9.05 | 1.67/1.18 | 3.72 |
| 4 | 947.75 | 300.0/303.4 | 0.75/0.26 | 12.99 | 0.82/0.23 | 6.17 |
| 5 | 947.75 | 300.0/303.7 | 0.75/0.26 | 12.99 | 0.82/0.22 | 8.14 |
| 6 | 947.75 | 300.0/304.7 | 0.75/0.26 | 12.99 | 0.84/0.21 | 7.07 |
| 7 | 1085.75 | 304.0/308.4 | 1.75/1.00 | 9.75 | 1.98/0.88 | 4.12 |
| 8 | 1085.75 | 304.0/308.4 | 1.75/1.00 | 9.75 | 1.98/0.88 | 4.59 |
| 9 | 1085.75 | 304.0/308.6 | 1.75/1.00 | 9.75 | 1.99/0.88 | 4.26 |
| 10 | 1085.75 | 310.9/315.3 | 2.00/0.75 | 9.10 | 2.21/0.64 | 4.63 |
| 11 | 1085.75 | 310.9/315.2 | 2.00/0.75 | 9.10 | 2.20/0.65 | 4.72 |
| 12 | 947.75 | 314.0/317.5 | 1.48/0.32 | 12.20 | 1.57/0.27 | 5.41 |
| 13 | 1085.75 | 317.5/320.4 | 2.21/0.54 | 9.15 | 2.33/0.48 | 4.37 |
| 14 | 1085.75 | 317.5/320.5 | 2.21/0.54 | 9.15 | 2.33/0.48 | 4.43 |
| 15 | 1085.75 | 323.0/325.8 | 2.35/0.40 | 9.15 | 2.44/0.36 | 3.77 |
| 16 | 1085.75 | 323.0/326.1 | 2.35/0.40 | 9.15 | 2.45/0.35 | 4.26 |
| 17 | 1085.75 | 327.0/329.9 | 2.43/0.32 | 9.25 | 2.51/0.28 | 3.52 |
| 18 | 947.75 | 331.0/332.2 | 1.86/0.14 | 10.40 | 1.88/0.13 | 3.86 |
| 19 | 947.75 | 331.0/332.5 | 1.86/0.14 | 10.40 | 1.88/0.13 | 3.92 |
| 20 | 947.75 | 331.0/332.5 | 1.86/0.14 | 10.40 | 1.88/0.13 | 3.83 |
| 21 | 947.75 | 293.9/298.9 | 0.72/0.40 | 9.88 | 0.83/0.35 | 6.48 |
| 22 | 947.75 | 293.9/299.3 | 0.72/0.40 | 9.88 | 0.84/0.34 | 7.82 |
| 23 | 947.75 | 293.9/298.0 | 0.72/0.40 | 9.88 | 0.81/0.35 | 7.48 |
| 24 | 947.75 | 293.9/297.4 | 0.72/0.40 | 24.88 | 0.80/0.36 | 8.99 |
| 25 | 947.75 | 293.9/297.2 | 0.72/0.40 | 24.88 | 0.79/0.36 | 8.85 |
| 26 | 947.75 | 293.9/297.2 | 0.72/0.40 | 24.88 | 0.79/0.36 | 7.84 |
| 27 | 947.75 | 294.5/300.6 | 0.87/0.55 | 49.58 | 1.04/0.47 | 9.20 |
| 28 | 947.75 | 294.5/300.6 | 0.87/0.55 | 49.58 | 1.04/0.47 | 9.40 |
| 29 | 947.75 | 294.5/300.5 | 0.87/0.55 | 49.58 | 1.04/0.47 | 9.10 |
| 30 | 947.75 | 294.5/299.6 | 0.87/0.55 | 77.58 | 1.01/0.48 | 6.86 |
| 31 | 947.75 | 294.5/299.8 | 0.87/0.55 | 77.58 | 1.02/0.48 | 7.59 |
| 32 | 947.75 | 294.5/299.4 | 0.87/0.55 | 77.58 | 1.01/0.48 | 8.53 |
| 33 | 947.75 | 294.5/298.5 | 0.87/0.55 | 101.58 | 0.98/0.50 | 6.32 |
| 34 | 947.75 | 294.5/298.4 | 0.87/0.55 | 101.58 | 0.98/0.50 | 5.43 |
| 35 | 947.75 | 294.5/298.2 | 0.87/0.55 | 101.58 | 0.97/0.50 | 6.26 |
| 36 | 947.75 | 294.5/297.0 | 0.87/0.55 | 203.58 | 0.94/0.52 | 4.50 |
| 37 | 947.75 | 294.5/296.9 | 0.87/0.55 | 203.58 | 0.93/0.52 | 4.91 |
| 38 | 947.75 | 294.5/297.0 | 0.87/0.55 | 203.58 | 0.94/0.52 | 5.17 |
| 39 | 947.75 | 294.5/298.3 | 0.99/0.72 | 388.29 | 1.11/0.66 | 4.62 |
| 40 | 947.75 | 294.5/297.0 | 0.99/0.72 | 388.29 | 1.07/0.68 | 3.80 |
| 41 | 947.75 | 294.5/298.2 | 0.99/0.72 | 388.29 | 1.11/0.66 | 4.51 |
| 42 | 947.75 | 294.5/296.7 | 0.99/0.72 | 604.29 | 1.06/0.68 | 3.55 |
| 43 | 947.75 | 294.5/296.3 | 0.99/0.72 | 604.29 | 1.05/0.69 | 3.22 |
| 44 | 947.75 | 294.5/296.2 | 0.99/0.72 | 604.29 | 1.05/0.69 | 3.24 |
| 45 | 1085.75 | 294.0/299.4 | 1.33/1.37 | 20.30 | 1.60/1.23 | 4.90 |
| 46 | 1085.75 | 294.0/298.2 | 1.33/1.37 | 20.30 | 1.54/1.26 | 4.93 |
| 47 | 1085.75 | 294.0/298.9 | 1.33/1.37 | 20.30 | 1.58/1.24 | 4.95 |
| 48 | 1085.75 | 294.0/299.1 | 1.33/1.37 | 77.30 | 1.59/1.24 | 4.50 |
| 49 | 1085.75 | 294.0/298.9 | 1.33/1.37 | 77.30 | 1.58/1.24 | 4.67 |
| 50 | 1085.75 | 294.0/298.8 | 1.33/1.37 | 235.30 | 1.57/1.25 | 3.93 |
| 51 | 1085.75 | 294.0/298.9 | 1.33/1.37 | 235.30 | 1.58/1.24 | 3.97 |
| 52 | 1085.75 | 294.0/296.6 | 1.33/1.37 | 442.30 | 1.46/1.30 | 3.79 |
| 53 | 1085.75 | 294.0/296.9 | 1.33/1.37 | 442.30 | 1.48/1.29 | 3.75 |
| 54 | 1085.75 | 294.8/298.8 | 0.77/0.43 | 4.49 | 0.87/0.38 | 7.72 |
| 55 | 1085.75 | 295.0/298.2 | 0.80/0.45 | 7.05 | 0.88/0.41 | 6.85 |
| 56 | 1085.75 | 295.0/298.2 | 0.80/0.45 | 7.05 | 0.88/0.41 | 7.81 |
| 57 | 1085.75 | 295.0/298.2 | 0.80/0.45 | 7.05 | 0.88/0.41 | 7.60 |
| 58 | 1085.75 | 295.0/299.6 | 1.39/1.36 | 14.25 | 1.63/1.24 | 5.04 |
| 59 | 1085.75 | 295.0/299.5 | 1.39/1.36 | 14.25 | 1.62/1.24 | 4.78 |
| 60 | 1085.75 | 295.0/299.6 | 1.39/1.36 | 14.25 | 1.62/1.24 | 4.76 |
| 61 | 974.63 | 293.8/302.1 | 0.85/0.57 | 1.48 | 1.09/0.45 | 4.84 |
| 62 | 974.63 | 293.8/302.1 | 0.85/0.57 | 1.48 | 1.09/0.45 | 5.52 |
| 63 | 974.63 | 293.8/301.7 | 0.85/0.57 | 1.48 | 1.08/0.46 | 5.37 |
| 64 | 974.63 | 293.8/302.3 | 0.85/0.57 | 3.68 | 1.11/0.44 | 4.44 |
| 65 | 974.63 | 293.8/302.5 | 0.85/0.57 | 3.68 | 1.10/0.44 | 4.31 |
| 66 | 974.63 | 293.8/302.2 | 0.85/0.57 | 3.68 | 1.09/0.45 | 4.44 |
| 67 | 974.63 | 293.8/302.9 | 0.85/0.57 | 8.68 | 1.11/0.44 | 3.89 |
| 68 | 974.63 | 293.8/302.9 | 0.85/0.57 | 8.68 | 1.11/0.44 | 3.83 |
| 69 | 974.63 | 293.8/303.4 | 0.85/0.57 | 8.68 | 1.12/0.43 | 3.78 |
| 70 | 974.63 | 293.8/302.6 | 0.95/0.70 | 98.35 | 1.24/0.56 | 1.14 |
| 71 | 974.63 | 293.8/298.4 | 0.95/0.70 | 98.35 | 1.10/0.63 | 0.84 |
| 72 | 974.63 | 294.5/301.4 | 1.03/0.77 | 3.03 | 1.27/0.65 | 3.79 |
| 73 | 974.63 | 294.5/300.5 | 1.03/0.77 | 3.03 | 1.24/0.67 | 3.82 |
| 74 | 974.63 | 294.5/300.5 | 1.03/0.77 | 3.03 | 1.24/0.67 | 3.81 |
| 75 | 974.63 | 294.5/300.6 | 1.03/0.77 | 10.20 | 1.24/0.67 | 3.46 |
| 76 | 974.63 | 294.5/300.5 | 1.03/0.77 | 10.20 | 1.24/0.67 | 3.16 |

**Table I** (Continued)

| run no. | $\lambda_{CO_2}$ ($cm^{-1}$)[a] | $T_0/T_f$ (K) | $P_0$ (Torr) monomer/dimer | diluent[b] $P$ (Torr) | $P_f$ (Torr) monomer/dimer | $10^6\tau$ (s) |
|---|---|---|---|---|---|---|
| 77 | 974.63 | 294.5/300.2 | 1.03/0.77 | 10.20 | 1.23/0.67 | 3.26 |
| 78 | 974.63 | 294.5/299.9 | 1.03/0.77 | 27.20 | 1.22/0.68 | 2.54 |
| 79 | 974.63 | 294.5/299.5 | 1.03/0.77 | 27.20 | 1.20/0.69 | 2.40 |
| 80 | 974.63 | 294.5/299.4 | 1.03/0.77 | 27.20 | 1.20/0.69 | 2.50 |
| 81 | 974.63 | 293.5/298.6 | 0.88/0.62 | 4.10 | 1.03/0.55 | 5.35 |
| 82 | 974.63 | 293.5/298.3 | 0.88/0.62 | 4.10 | 1.02/0.55 | 5.50 |
| 83 | 974.63 | 293.5/297.9 | 0.88/0.62 | 4.10 | 1.01/0.56 | 5.48 |
| 84 | 974.63 | 293.5/297.4 | 0.88/0.62 | 11.00 | 0.99/0.56 | 4.28 |
| 85 | 974.63 | 293.5/297.2 | 0.88/0.62 | 11.00 | 0.99/0.57 | 4.56 |
| 86 | 974.63 | 293.5/296.8 | 0.88/0.62 | 11.00 | 0.98/0.57 | 4.44 |
| 87 | 974.63 | 293.5/296.2 | 0.88/0.62 | 20.00 | 0.96/0.58 | 3.97 |
| 88 | 974.63 | 293.5/296.3 | 0.88/0.62 | 20.00 | 0.96/0.58 | 3.22 |
| 89 | 974.63 | 293.5/296.1 | 0.88/0.62 | 20.00 | 0.96/0.58 | 3.80 |
| 90 | 974.63 | 293.5/295.9 | 0.88/0.62 | 29.00 | 0.95/0.59 | 2.56 |
| 91 | 974.63 | 293.5/295.4 | 0.88/0.62 | 29.00 | 0.94/0.59 | 2.75 |
| 92 | 974.63 | 293.5/295.3 | 0.88/0.62 | 29.00 | 0.93/0.59 | 3.00 |
| 93 | 974.63 | 293.5/297.4 | 0.94/0.71 | 3.74 | 1.07/0.65 | 4.42 |
| 94 | 974.63 | 293.5/301.8 | 0.94/0.71 | 3.74 | 1.21/0.57 | 4.51 |
| 95 | 974.63 | 293.5/301.6 | 0.94/0.71 | 3.74 | 1.21/0.58 | 4.57 |
| 96 | 974.63 | 293.5/303.7 | 0.94/0.71 | 8.10 | 1.27/0.54 | 4.78 |
| 97 | 974.63 | 293.5/303.5 | 0.94/0.71 | 8.10 | 1.28/0.54 | 4.82 |
| 98 | 974.63 | 293.5/303.1 | 0.94/0.71 | 8.10 | 1.26/0.55 | 4.55 |
| 99 | 974.63 | 293.5/303.7 | 0.94/0.71 | 12.35 | 1.28/0.54 | 3.98 |
| 100 | 974.63 | 293.5/303.3 | 0.94/0.71 | 12.35 | 1.26/0.55 | 4.20 |
| 101 | 974.63 | 293.5/303.4 | 0.94/0.71 | 12.35 | 1.25/0.55 | 4.17 |
| 102 | 974.63 | 293.5/304.3 | 0.94/0.71 | 28.35 | 1.29/0.53 | 3.39 |
| 103 | 974.63 | 293.5/304.1 | 0.94/0.71 | 28.35 | 1.29/0.54 | 3.40 |
| 104 | 974.63 | 293.5/303.7 | 0.94/0.71 | 28.35 | 1.28/0.54 | 2.95 |

[a] Average energy 750 mJ for all lines used. Absorbence of $CO_2$ laser irradiation was ≤10 mJ for all runs. [b] For runs 1–60 argon was the diluent; for runs 61–71 acetone-$d_6$ was used; for runs 72–80 THF-$d_8$ was used; for runs 81–92 ethylene oxide was used; and for runs 93–104 trimethylene oxide was used.

somewhat due to transfer of populations from the ground of $\nu_{18}$ to higher states. Let $\hat{g}(E)$ be the computed vibrational state density, not counting $\nu_{18}$(C–H). Then the fraction of all molecules which remain in the ground $\nu_{18}$ state, at any temperature is

$$\frac{\hat{N}_{18}}{N_{\text{total}}} = \frac{\int \hat{g} \exp(-E/RT)\, dE}{\int g \exp(-E/RT)\, dE} \qquad (5)$$

Comparison of this ratio for $T_0 = 300$ K versus $T_0 + \Delta T = 305$ K (0.99962 vs 0.99958) shows that there is an insignificant decrement in the ground-state population for a small change in temperature due to the statistical redistribution among the vibrational states of the dimer. We estimated this redistribution takes place on a time scale of $\ll 5$ μs (at 2 Torr of formic acid) and should be essentially temperature independent over the short range used in these T-jump experiments. On a longer time scale, the dimer–monomer relaxation adjusts to the compositions appropriate for the higher temperature. Clearly, the dissociation process occurs from vibrationally excited dimers and these populations incorporate very few molecules that are not in the $\nu_{18}$ ground state.

Lifetimes of the transient reacting species must be derived from specific mechanisms. An initial test is application of RRKM theory for a unimolecular process.

**I.** Suppose the mechanism was

$$\phi \overset{(X)}{\rightleftharpoons} \Omega \rightleftharpoons 2\Gamma$$

Assuming no additional excitation is required for the second step, one anticipates $E_0 \approx 12$ kcal/mol on the basis of

$$E_0 = \Delta H^\circ_0 = \Delta H^\circ_T - \int_0^T [C_p(2\Gamma) - C_p(\phi)]\, dT \qquad (6)$$

In this model, species Ω with vibrational energy content less than 12 kcal is merely a particular group of states of the energized $\phi$. Basic to RRKM is the assumption that intramolecular vibrational energy flow is very rapid (on a time scale of ps). The postulated geometry and vibrational frequencies of the transition structure (assumed to be "loose")[18] are listed in Table II. $k_{uni}$ values versus

**Table II.** Parameters for RRKM Calculations ($\phi \rightarrow 2\Gamma$)

| $\phi$ | transition structure | $\phi$ | transition structure |
|---|---|---|---|
| | Moments of Inertia | | |
| 84.30 | 83.85 | 289.61 | 436.36 |
| 205.31 | 352.51 | | |
| | Frequencies | | |
| 3110 (2) | 3339 (2) | 1062 | 1043 |
| 2938 (2) | 2957 (2) | 997 | 810 |
| 1745 | 1765 | 917 | 780 |
| 1736 | 1723 | 697 | 660 |
| 1450 | 1450 | 675 | 650 |
| 1395 | 1395 | 262 | rxn coord |
| 1365 | 1365 | 237 | 200 |
| 1350 | 1350 | 190 | 180 |
| 1217 | 1160 | 172 | 115 |
| 1204 | 1160 | 160 | 80 |
| 1063 | 1044 | 100 | 50 |

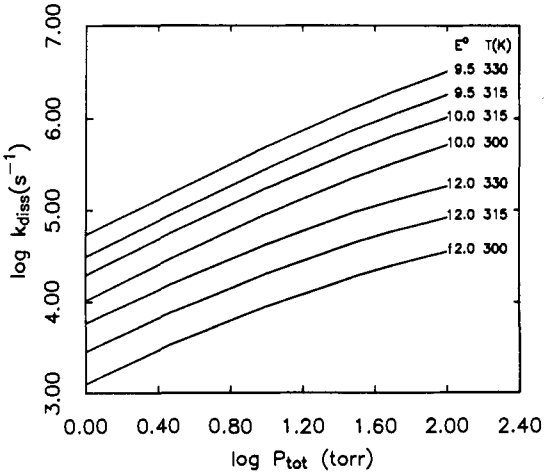


**Figure 7.** RRKM plots of log $k_{uni}$ versus log $P$, with argon as the buffer gas ($\lambda_{Ar} = 0.1$). The solid lines are $k_{uni}$ pressure-dependent values for the indicated temperatures and $E_0$'s.

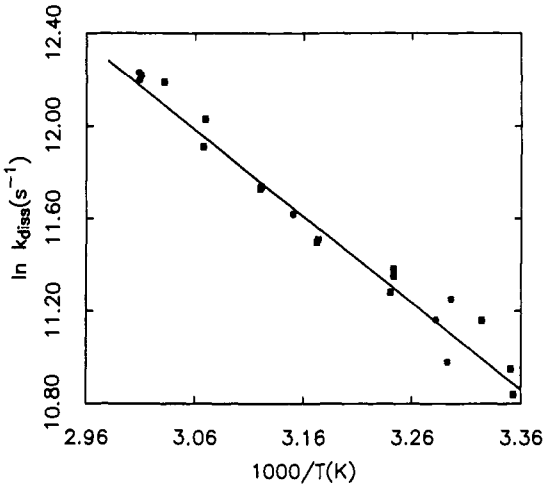


**Figure 8.** Arrhenius plot for the dissociation of formic acid dimer. $E_a$ = 7.4 ± 1.0 kcal/mol; ln $A$ = 23.43. (●) Dimer irradiated; (■) monomer irradiated.

**Table III.** Tabulated Values of $k_{diss}$ at Various Temperatures[a]

| | | $10^{-4}k_{diss}$ ($s^{-1}$) | | | | $10^{-4}k_{diss}$ ($s^{-1}$) | |
|---|---|---|---|---|---|---|---|
| run no. | $T_f$ (K) | eq 6 | eq 8 | run no. | $T_f$ (K) | eq 6 | eq 8 |
| 1 | 298.2 | 5.12 | 5.31 | 11 | 315.3 | 9.98 | 10.4 |
| 2 | 298.4 | 5.71 | 5.92 | 12 | 317.5 | 10.9 | 11.1 |
| 3 | 300.8 | 7.05 | 7.56 | 13 | 320.4 | 12.5 | 12.9 |
| 4 | 303.4 | 7.70 | 7.88 | 14 | 320.5 | 12.4 | 12.8 |
| 5 | 303.7 | 5.89 | 6.02 | 15 | 325.8 | 16.8 | 17.1 |
| 6 | 304.7 | 7.01 | 7.16 | 16 | 326.1 | 14.9 | 15.2 |
| 7 | 308.4 | 8.75 | 9.24 | 17 | 329.9 | 19.7 | 20.0 |
| 8 | 308.4 | 8.48 | 8.94 | 18 | 332.2 | 20.2 | 20.3 |
| 9 | 308.6 | 7.89 | 8.32 | 19 | 332.5 | 19.9 | 20.1 |
| 10 | 315.3 | 9.86 | 10.3 | 20 | 332.5 | 20.4 | 20.6 |

[a] Experimental conditions are given in Table I under the corresponding run number. Arrhenius fit parameters (eq 6) $E_a$ = 7.4 ± 1 kcal/mol, ln $A$ = 23.43; (eq 8) $E_a$ = 7.2 ± 1 kcal/mol, ln $A$ = 23.16.

total pressure are plotted in Figure 7 for a range of temperatures. At pressures less than 10 Torr the kinetics is in the second-order regime.[19] In converting the observed relaxation times to dissociation rate constants the following expression was used.

$$k_{dissoc}^{-1} = \tau_{exp}\{4K_{\Gamma\to\phi}^{(c)}[\Gamma] + 1\} \quad (7)$$

$$K_{\Gamma\to\phi}^{(c)} = (RT)^{-1}\exp(-39.24/R)\exp(+15250/RT)$$

This model is unacceptable because it predicts dissociation rate constants that are much too low. Even more impressive is the measured activation energy $E_a$ = 7.4 ± 1.0 kcal/mol, which is independent of whether the monomer or dimer band is irradiated (Table III and Figure 8). [We question the value 11.4 kcal/mol reported for acetic acid[7] on the basis of the $\Delta T$ values these investigators estimated for the reactant volumes probed by the He/Ne beam.]

The measured low activation energy clearly is not a consequence of a photon augmented process:

$$\phi + h\nu \rightarrow \phi^{(v)}$$

$$\phi^{(v)} + (X) \rightarrow 2\Gamma + (X)$$

Since the energy content of one Einstein of $CO_2$ laser radiation is about 3 kcal, *were every $\phi$ molecule to absorb a single photon*, and rapid IVR to apply, the entire distribution curve would be shifted to higher levels by 3 kcal, at most. That would be equivalent to a down-shift of the $k(E)$ curve by the same amount, leading to $E_{0(\phi\Gamma)}^{h\nu} \approx 9$ kcal/mol (Figure 6). The predicted $k_{uni}$ at 1 Torr is still too low, but more persuasive is the fact that for the low absorptions used in these experiments, the number of photons retained is less by 1–2 orders of magnitude than the number of dimers present.

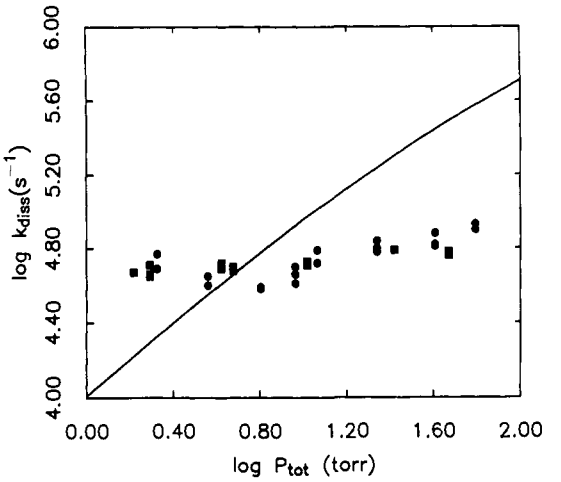


**Figure 9.** log $k_{uni}$ versus log $P_{total}$, with $P_{total} = P_{FA} + 0.1P_{Ar}$. The calculated curve is the RRKM prediction for $E_0$ = 10 kcal/mol, at 300 K. (●) Irradiated at 947.75 $cm^{-1}$ (dimer); (■) irradiated at 1085.75 $cm^{-1}$ (monomer).

**II.** The low activation energy suggests that the Ω configuration is a transient trap. Suppose the mechanism were

$$\phi + X \underset{1}{\overset{-1}{\rightleftharpoons}} \Omega + X$$

$$\Omega + X \underset{2}{\overset{-2}{\rightleftharpoons}} 2\Gamma + X$$

Since Ω reaches steady state rapidly

$$-\frac{d\phi}{dt} = k_1\phi X\frac{k_2}{k_{-1}+k_2} - \frac{k_{-1}k_{-2}\Gamma X}{k_1+k_2} \quad (8)$$

The relaxation expression for this case is

$$k_{diss}^{-1} = \tau_{exp}\frac{4[\Gamma]}{K_{\phi\to\Gamma}^{(c)} + K_{\phi\to\Omega}^{(c)}[\Gamma]} + 1 \quad (9)$$

$$K_{\phi\Omega}^{(c)} = K_{\phi\Omega}^{(p)} = \exp(22/R)\exp(-8500/RT)$$

The condition that $k_2 > k_{-1}$ is satisfied for $E^\circ_{\phi\to\Omega} \approx 9.5$ kcal/mol and $E^\circ_{\Omega\to\Gamma} \approx 5.5$ kcal/mol. In this model we assumed that there is a slight activation energy (≈1 kcal/mol) for return of Ω (with the broken bond) to $\phi$ status. This model is not acceptable, even though the expected activation energy is much closer to that observed, because the required second-order pressure dependence was not verified. Whereas for this model $k_{uni} = k_{bi}\{[\phi] + [\Gamma] + \lambda[Ar]\}$, we found no dependence on the Ar pressure over the range 10–600 Torr. Figure 9 illustrates the discrepancy between the predicted and observed $k_{uni}$'s, plotted under the assumption that the collision efficiency of Ar was 0.1 of formic acid. The indicated $\lambda(Ar) \approx 0$ is unacceptable.

**III.** The proportionately large discrepancy between the experimentally determined activation energy and the magnitude anticipated from the established $\Delta H^\circ_{diss}$ is reminiscent of similar discrepancies between spectroscopic $D_0$ values for many diatomics and the activation energies for their dissociation, as determined from shock tube experiments.[20] For three-body associations (in general) it is well established[21] that the rate constants decrease with rising temperature (negative $E_{a,ass}$). This is qualitatively,

(18) Wardlaw, D. M.; Marcus, R. A. *Chem. Phys. Lett.* **1984**, *110*, 230. Quack, M.; Troe, J. *Ber. Bunsen-Ges. Phys. Chem.* **1977**, *81*, 329.

(19) The correction for reversibility which should be incorporated into RRKM calculations [Bauer, S. H.; Lazaar, K. I. *J. Chem. Phys.* **1983**, *79*, 2808] is small for a dissociation/association process, since the density of states of the product species is much larger than that of the reacting species.

(20) Current review: Kern, R. D. *Compr. Chem. Kinet.* **1976**, *18*, 1.

(21) Kerr, J. A.; Moss, S. J., Eds. *Handbook of Bimolecular and termolecular Reactions*; CRC Press: Cleveland, 1981.

but not quantitatively, consistent with $E_{a,diss} < \Delta H°_{diss}$. The reason for negative $E_a$'s for radical recombinations is presumed to be due to more efficient energy removal by the third body when the temperature declines. Indeed, for near-resonant vibrational-energy transfers the cross section does rise with $T^{-1}$.[22] However, the formic acid data were taken very close to equilibrium conditions with almost negligible perturbations by the step rise in temperature. Its $E_a$ was evaluated over a small temperature range (≈50°) so that there is no signficant effect of temperature on the three-body efficiency. None-the-less, to account for both the low activation energy and the absence of the expected Ar pressure dependence there is merit in retaining the analogy between the kinetics of dissociation of formic acid and that of the dissociation of $I_2$ augmented by I atoms: $I + I_2 \rightarrow \{I_3\} \rightarrow 3I$.[23]

An acceptable mechanism consists of an association *displacement* followed by a rapid dissociation:

$$\phi \text{ or } \Gamma \overset{(X)}{\rightleftharpoons} (\phi \text{ or } \Gamma)^v \text{ (at EQ)}$$

$$(\phi + \Gamma)^v \underset{K_1}{\overset{K_{-1}}{\rightleftharpoons}} [T] \overset{\text{(fast)}}{\rightleftharpoons} \Omega + \Gamma$$

$$\Omega + X \underset{K_2}{\rightleftharpoons} 2\Gamma + X \text{ (fast)}$$

Structurally we visualize the following sequence Indeed, one may

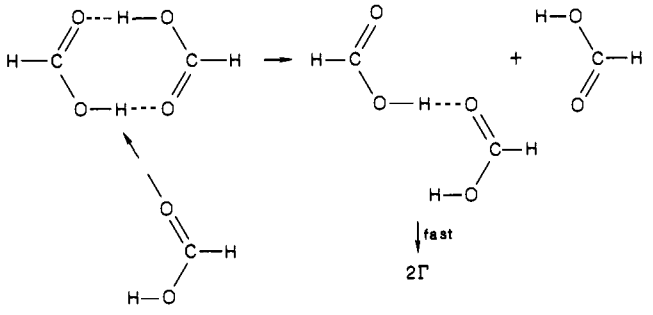


have anticipated that the conversion of $\phi$ to $\Omega$ via this route requires the lowest activation energy and that this path dominates over the *unassisted* ring opening by vibrational excitation through argon colliders. Also, since the monomer concentration increases only as the square root of the formic acid pressure, and the useful experimental range covers less than a factor of 3, irreproducibilities in the measurements of the relaxation times mask this effect; hence no direct pressure dependence on the formic acid could be established.

This model suggests that other strongly H-bonding species, of which substantial pressures can be added to this system, should appreciably decrease the relaxation time. However, these should have no significant absorptions either of He/Ne or $CO_2$ laser frequencies, so as not to upset the T-jump process nor the relaxation diagnostic. This eliminates alkyl ethers and alcohols. (The fully deuteriated species were not available.) Methyl alcohol not only absorbs the He/Ne frequency, but its polymers (dimers and tetramers[24]) also are dissociated by $CO_2$ laser light.[25] We measured the relative catalytic efficiences of per-deuterioacetone, trimethylene oxide, ethylene oxide, tetrahydrofurane-$d_8$, and water (Table IV). All show a linear dependence of the augmented dissociation rate constant on pressure of the diluent

$$k_{obsd} = k_{bi}^{\phi\Gamma}[\Gamma] + k_{bi}^{\phi X}[X] \qquad (10)$$

as illustrated in Figure 10. At 303 K, the intercept for $(CD_3)_2CO$ and THF-$d_8$ is $(8.9–9.1) \times 10^4$ s$^{-1}$, in agreement with corresponding values when Ar was the diluent. Water accelerated the rate, comparable to acetone, but these runs were difficult to reproduce quantitatively, due to adsorption on the glass lead lines. When the slopes of the ethylene and trimethylene oxides were converted to 303 K, the following sequence appeared:

$$(CD_3)_2CO \quad k_{bi}^{\phi X} = 2.69 \times 10^3 \text{ s}^{-1} \text{ Torr}^{-1}$$

$$(CH_2)_2O \quad k_{bi}^{\phi X} = 2.26 \ (1.76\times 10^3 \text{ s}^{-1} \text{ at 297 K})$$

$$(CH_2)_3O \quad k_{bi}^{\phi X} = 2.03 \ (1.80\times 10^3 \text{ s}^{-1} \text{ at 300 K})$$

$$\text{THF-}d_8 \quad k_{bi}^{\phi X} = 1.63 \times 10^3$$

These values measure relative OHO bonding strengths.

The temperature dependence of the principal "bimolecular" rate constant may be expressed in the form

**Table IV.** Dissociation Rate Constants for the Case of Added Acetone-$d_6$ and THF-$d_8$

| acetone-$d_6$[a] | | | THF-$d_8$[b] | | |
|---|---|---|---|---|---|
| $[D_3CC(O)CD_3]$ (Torr) | $10^{-4}k_{diss}$ (s$^{-1}$) eq 6 | eq 8 | $[C_4D_8O]$ (Torr) | $10^{-4}k_{diss}$ (s$^{-1}$) eq 6 | eq 8 |
| 1.48 | 7.79 | 8.14 | 3.03 | 8.68 | 9.18 |
| 1.48 | 6.83 | 7.14 | 3.03 | 8.33 | 8.83 |
| 1.48 | 6.93 | 7.24 | 3.03 | 8.34 | 8.84 |
| 3.68 | 8.72 | 9.10 | 10.20 | 9.24 | 9.79 |
| 3.68 | 8.91 | 9.31 | 10.20 | 10.1 | 10.7 |
| 3.68 | 8.54 | 8.93 | 10.20 | 9.72 | 10.3 |
| 8.68 | 10.0 | 10.4 | 27.20 | 12.2 | 13.0 |
| 8.68 | 10.2 | 10.6 | 27.20 | 12.8 | 13.5 |
| 8.68 | 10.5 | 10.9 | 27.20 | 12.2 | 13.0 |
| 98.35 | 31.4 | 33.0 | | | |
| 98.35 | 36.4 | 38.5 | | | |

| ethoxide[c] | | | oxetane[d] | | |
|---|---|---|---|---|---|
|  (Torr) | $10^{-4}k_{diss}$ (s$^{-1}$) eq 6 | eq 8 |  (Torr) | $10^{-4}k_{diss}$ (s$^{-1}$) eq 6 | eq 8 |
| 4.10 | 6.02 | 6.35 | 3.74 | 6.63 | 7.04 |
| 4.10 | 5.80 | 6.11 | 3.74 | 7.69 | 8.10 |
| 4.10 | 5.73 | 6.04 | 3.74 | 7.54 | 7.94 |
| 11.00 | 7.18 | 7.58 | 8.10 | 7.77 | 8.16 |
| 11.00 | 6.68 | 7.05 | 8.10 | 7.66 | 8.06 |
| 11.00 | 6.78 | 7.16 | 8.10 | 8.00 | 8.42 |
| 20.00 | 7.39 | 7.82 | 12.35 | 9.36 | 9.83 |
| 20.00 | 9.14 | 9.66 | 12.35 | 8.74 | 9.18 |
| 20.00 | 7.69 | 8.13 | 12.35 | 8.81 | 9.26 |
| 29.00 | 11.3 | 11.9 | 28.35 | 11.2 | 11.8 |
| 29.00 | 10.3 | 10.9 | 28.35 | 11.1 | 11.7 |
| 29.00 | 9.4 | 10.0 | 28.35 | 12.6 | 13.2 |

[a] Experimental conditions are listed in Table I, runs 61–71. [b] Experimental conditions are listed in Table I, runs 72–80. [c] Experimental conditions are listed in Table I, runs 81–92. [d] Experimental conditions are listed in Table I, runs 93–104.

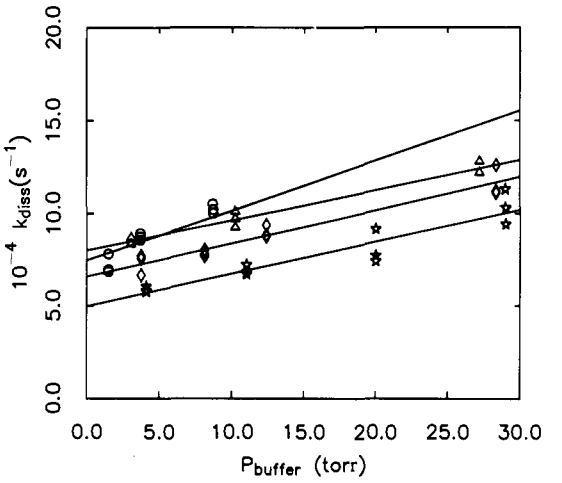


**Figure 10.** The catalytic effect of added O···HO forming species on the dissociation rate constant of formic acid: (○) $(CD_3)_2CO$ at 303 K [two points (41:35) at 100 Torr not shown]; (△) THF-$d_8$ at 303 K; (◇) $(CH_2)_3O$ at 300 K; (☆) $(CH_2)_2O$ at 297 K.

(22) Sharma, R. D.; Brau, C. A. *J. Chem. Phys.* **1969**, *50*, 924. Dillon, T. A.; Stephenson, J. C. *Phys. Rev.* **1972**, *6*, 1460.
(23) Bunker, D. L.; Davidson, N. *J. Am. Chem. Soc.* **1958**, *80*, 5085, 5090.
(24) Renner, T. A.; Kucera, G. H.; Blander, M. *J. Chem. Phys.* **1977**, *66*, 177.
(25) Hoffbauer, M. A.; Grise, C. F.; Gentry, W. R. *J. Phys. Chem.* **1984**, *88*, 181.

$$K_1 = e^2\left(\frac{kT}{h}\right)\exp(\Delta S_c^*/R)\exp(-E_a/RT) \qquad (11)$$

$$E_a = 7.40 \text{ kcal/mol}; \ \Delta S^*_c = 17.6 \text{ eu}$$

This entropy of activation is consistent with the assumed value $\Delta S^\circ_{\phi\Omega} \approx 22$ eu.

## Conclusion

The T-jump technique for measuring relaxation times in the $\mu$s range allows one to investigate molecular conversions over low barriers and provides a means for exploring limits of applicability of classical kinetic formulations. The mechanism that accounts for the dissociation of formic acid dimer in the gas phase may have general applicability, since the process has a lower activation energy than the bond dissociation energy ($D_{AB}$) whenever $K_2 > K_{-1}$. At present there are too few examples to permit the development of empirical rules for predicting the relative magnitudes of these basic rate parameters. Clearly it is essential that there be significant coupling between the newly formed X–A bond and the dissociating A–B bond.

$$X + AB \underset{K_1}{\overset{K_{-1}}{\rightleftharpoons}} [XAB] \xrightarrow{\text{(fast)}} XA + B \qquad (12)$$
$$\qquad\qquad\qquad\qquad\qquad\qquad\quad \underset{K_2}{\longrightarrow} X + A$$

**Acknowledgment.** The investigation was supported by a grant from the AFOSR [F49620-84-C-0031].

**Registry No.** Formic acid, 64-18-6.

# Molecular-Beam Study of Chemiionization Reactions of $SbF_5$

**M. V. Arena,[†] J. F. Hershberger,[‡] J. J. McAndrew,[⊥] R. J. Cross,* and M. Saunders***

*Contribution from the Department of Chemistry, Yale University, New Haven, Connecticut 06511-8118.* *Received March 23, 1987*

**Abstract:** We have studied the energy dependence of the reactive cross sections for three sets of isomeric reactions, all involving the halide or electron transfer to antimony pentafluoride from organic halides. We find that the cross sections for iodide abstraction of the four butyl iodides have virtually the same energy dependence. This strongly suggests that some rearrangement takes place during the reactive collision so that the product in all cases is the stable *tert*-butyl cation. Similar studies on five-carbon acyl chlorides, however, show very different behavior when the resulting acyl cation decomposes by eliminating CO. Finally, results on the competition between halide abstraction and electron transfer from isomers of butenoyl chloride seem to indicate that the two processes do not pass through a common intermediate.

During the past few years we have used crossed molecular beams to study the dynamics of gas-phase chemiionization reactions of $SbF_5$ in order to understand their basic mechanisms. We have found two different classes of reactions. One is a halide abstraction[1-4]

$$SbF_5 + RX \rightarrow SbF_5X^- + R^+ \qquad (1)$$

where X is a halogen and R is an organic or inorganic group. The second is an electron transfer[5]

$$SbF_5 + B \rightarrow SbF_5^- + B^+ \qquad (2)$$

where B is an organic base. In each case we measured the angular and energy distributions of the product ions. In the case of reaction 1 the product distributions have forward–backward symmetry about the center of mass. This indicates that the reaction proceeds by way of a long-lived complex that sticks together for a rotational period or longer. At the highest available energy, 6.8 eV, the distributions begin to lose this symmetry. This may indicate that at higher energies the lifetime of the complex becomes comparable to the rotational period. Unfortunately, the asymmetry is only just larger than the experimental error, and we cannot go to a higher energy where the lifetime should be still shorter.

In contrast, the product angular and energy distributions for reaction 2 show no such symmetry except for the lowest energy studied. The reaction appears to go by way of a fast, direct mechanism. Our data are explained by a simple model. The two reactants are assumed to collide at large impact parameters, a grazing collision. The electron jumps from B to $SbF_5$. As the products separate, they are attracted to each other by the Coulomb force. The threshold energy should be the vertical ionization potential of B minus the vertical electron affinity of $SbF_5$. Because the reaction takes place in a grazing collision, there is very little internal energy transferred except that which is put into the molecules by the vertical electron jump. All translational energy in the reactants above the vertical threshold should go into translational energy of the products. We found this to be true for the reaction of $SnCl_4$, where the electron affinity is known, and tetrakis(dimethylamino)ethylene (TDMAE), which has one of the lowest ionization potentials of all organic molecules. The electron affinity of $SbF_5$ was unknown, but we obtained the same value at three different beam energies. Below the vertical threshold the electron-transfer reaction appears to go by way of a long-lived complex.

We have recently reconfigured the apparatus to study the total reactive cross section as a function of the amount and type of initial energy.[4] For reaction 1 the cross section rises rapidly above a threshold energy which is typically a few eV and depends on the RX species being studied. Well above the threshold energy, the effect of vibrational energy on the cross section is comparable to or less than that of translational energy. However, near the threshold, the effect of a small amount of vibrational energy may be comparable to that of several times as much translational

[†] Present address: Department of Chemistry, Stanford University, Stanford, CA 94305.
[‡] Present address: Department of Chemistry, Columbia University, New York, NY 10027.
[⊥] Present address: Department of Chemistry, Brookhaven National Laboratory, Upton, NY 11973.

(1) Auerbach, A.; Cross, R. J.; Saunders, M. *J. Am. Chem. Soc.* **1978**, *100*, 4908.
(2) Lee, L.; Russell, J. A.; Su, R. T. M.; Cross, R. J.; Saunders, M. *J. Am. Chem. Soc.* **1981**, *103*, 5031.
(3) Russell, J. A.; Hershberger, J. F.; McAndrew, J. J.; Cross, R. J.; Saunders, M. *J. Phys. Chem.* **1984**, *88*, 4494.
(4) Hershberger, J. F.; McAndrew, J. J.; Cross, R. J.; Saunders, M. *J. Chem. Phys.* **1987**, *86*, 4916.
(5) Russell, J. A.; Hershberger, J. F.; McAndrew, J. J.; Cross, R. J.; Saunders, M. *J. Chem. Phys.* **1985**, *82*, 2240.

0002-7863/87/1509-6658$01.50/0 